J. Geogr. Sci. 2010, 20(6): 803-817
DOI: 10.1007/s11442-010-0812-7

Spatio-temporal variation of photosynthetically active radiation in China in recent 50 years

ZHU Xudong[1,2], *HE Honglin[1], LIU Min[1,2], YU Guirui[1], SUN Xiaomin[1], GAO Yanhua[1]

1. Key Laboratory of Ecosystem Network Observation and Modeling, Institute of Geographic Sciences and Natural Resources Research, CAS, Beijing 100101, China;
2. Graduate University of Chinese Academy of Sciences, Beijing 100049, China

Abstract: Based on long-term measurement data of weather/ecological stations over China, this paper calculated and produced annually- and seasonally-averaged Photosynthetically Active Radiation (PAR) spatial data from 1961 to 2007, using climatological calculations and spatialization techniques. The spatio-temporal variation characteristics of annually- and seasonally-averaged PAR spatial data over China in recent 50 years were analyzed with Mann-Kendall trend analysis method and GIS spatial analysis techniques. The results show that: (1) As a whole, the spatial distribution of PAR is complex and inhomogeneous across China, with lower PAR in the eastern and southern parts of China and higher PAR in the western part. Mean annual PAR over China ranges from 17.7 mol m^{-2} d^{-1} to 39.5 mol m^{-2} d^{-1}. (2) Annually- and seasonally-averaged PAR of each pixel over China are averaged as a whole and the mean values decline visibly with fluctuant processes, and the changing rate of annually-averaged PAR is –0.138 mol m^{-2} d^{-1}/10a. The changing amplitudes among four seasons are different, with maximum dropping in summer, and the descending speed of PAR is faster before the 1990s, after which the speed slows down. (3) The analysis by each pixel shows that PAR declines significantly (α=0.05) in most parts of China. Summer and winter play more important roles in the interannual variability of PAR. North China is always a decreasing zone in four seasons, while the northwest of Qinghai-Tibet Plateau turns to be an increasing zone in four seasons. (4) The spatial distributions of the interannual variability of PAR vary among different periods. The interannual variabilities of PAR in a certain region are different not only among four seasons, but also among different periods.

Keywords: Photosynthetically Active Radiation (PAR); Mann-Kendall trend analysis; China

1 Introduction

Solar radiation is the most important source of energy required for plant growth. Solar radia-

Received: 2010-04-13 **Accepted:** 2010-05-08
Foundation: National Natural Science Foundation of China, No.41071251; National Basic Research Program of China, No.2010CB833504; Knowledge Innovation Program of the Chinese Academy of Sciences, No.KZCX2-YW-433-06; Information Project of the Chinese Academy of Sciences
Author: Zhu Xudong (1985–), Master Candidate, specialized in climate change & carbon cycle. E-mail: ecopig@163.com
***Corresponding author:** He Honglin (1971–), Associate Professor, E-mail: hhonglin@cern.ac.cn

tion with wavelengths between 400 and 700 nanometers (nm), which is called Photosynthetically Active Radiation (PAR), can be utilized by the plant biochemical processes in photosynthesis to convert light energy into biomass (Udo and Aro, 1999; Jacovides *et al.*, 2004). As a significant ecological factor influencing plant growth, PAR is a key parameter in photosynthesis modeling, vegetation primary productivity calculation, and in studies of ecosystem-atmosphere CO_2 exchange (Cao *et al.*, 2005). Monteith suggested that net primary production (NPP) under non-stressed conditions is linearly related to the amount of PAR that is absorbed by the green foliage (Monteith, 1972; Monteith, 1977). Absorbed PAR is the product of incident PAR and absorption coefficient (*f*PAR). Therefore, the variabilities of PAR at temporal and spatial scales directly influence the spatio-temporal variability of NPP. PAR is a significant climatic factor, and analyzing and detecting long-term changing trend of climatic factors is an important part of climate change research in the context of global climate change. Also, the study of the spatio-temporal variability of PAR can lend great support to the study on how the variability of PAR influences the process of photosynthesis in ecosystems (Graham *et al.*, 2003).

There are two measuring systems for PAR: one is radiation flux density (W m^{-2}), acquired from indirect measurement; the other is photosynthetic photon flux density (μmol m^{-2} s^{-1}), directly measured with a quantum sensor (Udo and Aro, 1999; Ross and Sulev, 2000). These two measuring systems can be interconvertible with a conversion coefficient of 4.57 μmol J^{-1} (Dye, 2004). A large amount of research work on the methods of estimating PAR has been performed by far; however, there are relatively less studies focusing on the spatio-temporal variation characteristics of PAR. Zhou *et al.* (1996) investigated the relationships between PAR and other meteorological factors, and introduced an estimation method of PAR based on global radiation. The variation characteristics of PAR in Qinghai-Tibet Plateau (Zhang *et al.*, 1997; Zhang *et al.*, 2000), Liaoning (Liu *et al.*, 2002), Tai Lake (Zhang and Qin, 2002), and Inner Mongolia (Bai and Wang, 2004) had been explored and local empirical estimation equations of PAR had been built. Hu *et al.* (2007) analyzed the variabilities of PAR in different regions across China, based on PAR observatory data from Chinese Ecosystem Research Network (CERN) field stations, and systematically explored the spatio-temporal variation characteristics of PAR over China. However, all of these studies focused on the spatio-temporal variability of PAR at site scale, hardly referring to regional scale. In recent years, with the increase in PAR observation stations, accumulation of PAR observatory data provides abundant data for the spatio-temporal variation characteristics analysis of PAR. In addition, the rapid development and wide application of GIS techniques make it possible for visualization analysis of the spatio-temporal variation characteristics of PAR.

This paper aims to explore the spatio-temporal variation characteristics of PAR at regional scale and reveal temporal dynamic characteristics and spatial evolution pattern of PAR, which will lay the foundation for further analysis of the impact of PAR variability on primary productivity of terrestrial ecosystems in China. Based on long-term measurement data of weather/ecological stations over China, we calculated and produced annually- and seasonally-averaged PAR spatial data from 1961 to 2007, using climatological calculation and spatialization techniques. Moreover, the spatio-temporal variation characteristics of annually- and seasonally-averaged PAR spatial data over China in recent 50 years were analyzed

with Mann-Kendall trend analysis method and GIS spatial analysis techniques.

2 Data and methods

2.1 Research data

Research Data using in this paper include climatic data and topographic data. Three climatic datasets are selected to calculate and spatialize PAR: (1) daily sunshine duration data observed at 740 weather stations across China for 1961–2007, provided by China Meteorological Administration; (2) daily global radiation and daily sunshine duration data observed at 122 radiation stations across China for 1961–2000, provided by China Meteorological Administration; (3) daily global radiation and daily PAR data observed at 36 field stations across China for 2004–2007, provided by CERN (Figure 1). DEM data (Digital Elevation Model) with a spatial resolution of 500 m×500 m, provided by Institute of Geographic Sciences and Natural Resources Research, is selected as topographic data for the spatial interpolation of PAR.

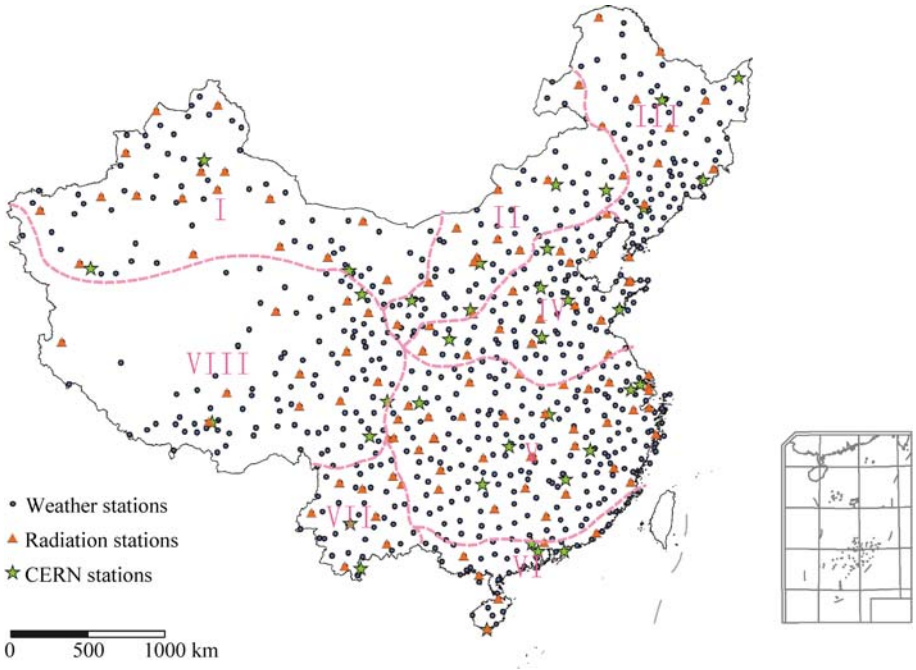

Figure 1 Spatial distribution of observation stations over China
(I. Northwest China; II. Inner Mongolia; III. Northeast China; IV. North China; V. Central China; VI. South China; VII. Southwest China; VIII. Qinghai-Tibet Plateau)

2.2 Calculation and spatialization methods of PAR

There are two main methods for calculation and spatialization of PAR: remote sensing retrieval (Van and Sanchez-Azofeifa, 2005) and data simulation based on ground observation (Lin *et al.*, 2002). According to spatial distribution of PAR observation stations and China's Physical Geography Division (Zhao and Chen, 1999), we divide China into eight regions:

Northwest China, Inner Mongolia, Northeast China, North China, Central China, South China, Southwest China, and Qinghai-Tibet Plateau (Figure 1). Based on two empirical equations of PAR vs. global radiation and global radiation vs. sunshine duration, we utilize PAR observatory data and ancillary meteorological data in a certain region to calculate PAR spatial data in this region, using ANUSPLIN spatial interpolation arithmetic. The entire calculation process is divided into three steps:

(1) Based on the empirical relationship between global radiation and sunshine duration described by Angstrom equation (Equation 1) (Ångstrøm, 1924), we firstly use global radiation and sunshine duration observatory data at 122 radiation stations across China to estimate coefficients (a, b) of Angstrom equations in eight regions (Table 1). Then, we utilize sunshine duration data from 740 weather stations across China to calculate global radiation of all these weather stations (He *et al.*, 2003; 2004a; 2004b).

$$\frac{Q}{Q'} = a + b\frac{n}{N} \tag{1}$$

where Q, Q' represent global radiation and extraterrestrial radiation respectively; n, N represent actual sunshine duration and possible sunshine duration respectively; and a, b are undetermined coefficients. Extraterrestrial radiation and possible sunshine duration can be derived from geographic latitude and day series (Tong *et al.*, 2005).

(2) ANUSPLIN arithmetic (Hutchinson, 1991; Hutchinson, 1995; Hutchinson, 2002) is selected for spatial interpolation of PAR over China (10 km×10 km). ANUSPLIN is a thin plate smoothing spline based spatial interpolation package that allows the use of multiple covariates as linear sub-models in addition to the independent spline variables (Hutchinson, 2002). It was developed by Australian National University and has been widely used in spatial interpolation of meteorological data (Hutchinson, 1991; Hijmans *et al.*, 2005). The influencing factors we take into account in the spatial interpolation of PAR include latitude, longitude and elevation.

(3) Based on the empirical relationship between photosynthetically active coefficient (η, PAR/Q) and clearness index (Q/Q') (Equation 2) (He *et al.*, 2004a; Yu *et al.*, 2004), we utilize PAR and global radiation observation data at 36 CERN field stations to estimate coefficients (c, d) of Equation 2 in eight regions, by means of parameter estimation with observatory data in respective regions (Table 1). And then we calculate η of each pixel over China, from which PAR spatial data is derived.

$$\eta = c + d\ln\frac{Q}{Q'} \tag{2}$$

Table 1 Estimated values of parameters of Equations (1) and (2) in different regions across China

Parameters	Ⅰ Northwest China	Ⅱ Inner Mongolia	Ⅲ Northeast China	Ⅳ North China	Ⅴ Central China	Ⅵ South China	Ⅶ Southwest China	Ⅷ Qinghai-Tibet Plateau
a	0.2590	0.1780	0.1928	0.1904	0.1519	0.1614	0.2019	0.2230
b	0.4779	0.5765	0.5373	0.5103	0.5739	0.5399	0.5354	0.5763
c	0.3610	0.3891	0.3549	0.3767	0.3712	0.3826	0.3742	0.3963
d	–0.0414	–0.0325	–0.0491	–0.0381	–0.0412	–0.0497	–0.0367	–0.0478

where Q, Q' represent global radiation and extraterrestrial radiation respectively; η represents photosynthetically active coefficient; and c, d are undetermined coefficients.

The comparison between parameters of eight regions (Table 1) and results of other research work (He *et al.*, 2004a; Sun *et al.*, 1992) indicates a slight difference in parameter values. However, the overall trends are quite consistent. The mean values of parameter a and b of eight regions (0.20, 0.54) are very close to the mean values for China as a whole (0.19, 0.55) reported by Sun *et al.* (1992), and nearly the same as those reported by some foreign literatures (Louche *et al.*, 1991; Almorox and Hontoria, 2004). Moreover, the mean values of parameter c and d are also close to those (0.40, –0.03) reported by He *et al.* (2004a). The differences among these estimated parameter values possibly attribute to the use of meteorological data in different years. The ultimately derived PAR spatial dataset covers land area of China and spans from 1961 to 2007, with a spatial resolution of 10 km×10 km and a temporal resolution of daily. Daily PAR data are calculated as annually- and seasonally-averaged PAR spatial data for the following analysis.

2.3 Time-varying analysis method of PAR

The time series of PAR spatial data are analyzed at pixel and regional scales respectively, using the Mann-Kendall trend analysis method. Rank-based Mann-Kendall trend analysis method is one of the non-parametric statistical test methods (also called distribution-free test methods), having significant advantages compared to traditional parametric statistical test methods. This non-parametric method allows inquiring on the presence of a tendency in long-term meteorological data, without having to make an assumption about its distributional properties. Moreover, this test is less influenced by the presence of outliers in the data and relatively easy to calculate (Wei, 2007). Therefore, Mann-Kendall trend analysis method has been widely used in time-varying analysis, and recommended by WMO (World Meteorological Organization) in time-varying analysis of environmental data (Yu *et al.*, 2002). The details of this statistical test method are as follows:

$$Z=\begin{cases}\dfrac{S-1}{\sqrt{Var(S)}} & (S>0)\\ 0 & (S=0)\\ \dfrac{S+1}{\sqrt{Var(S)}} & (S<0)\end{cases} \qquad S=\sum_{i=1}^{n-1}\sum_{j=i+1}^{n} sign(x_j-x_i) \qquad sign(\theta)=\begin{cases}1 & (\theta>0)\\ 0 & (\theta=0)\\ -1 & (\theta<0)\end{cases} \tag{3}$$

where Z is standardized test statistic; S is test statistic; x denotes the data values at times i and j; and n is the length of the data set. The statistic S is approximately normally distributed when $n \geqslant 8$, with mean and variance as follows:

$$E(S)=0 \tag{4}$$

$$Var(S)=\frac{n(n-1)(2n+5)-\sum_{p=1}^{q} t_p(t_p-1)(2t_p+5)}{18} \tag{5}$$

where q is the number of tied groups (a tied group is a set of sample data having the same value); t_p is the number of data points in the pth group; and n is the length of the data set.

The standardized test statistic Z has a mean of 0 and a standard deviation of 1. The hypothesis that no trend exists is declined (i.e. the trend varies significantly) if $|Z| > Z_{1-\alpha/2}$. $Z_{1-\alpha/2}$ refers to the corresponding value in normal distribution function table with confidence level at α.

The non-parametric robust estimate of the magnitude of the slope of linear trend (β) is given by

$$\beta = Median\left[\frac{x_j - x_i}{j - i}\right] \tag{6}$$

where x denotes the data values at times i and j. The trend is said to be decreasing if β is negative, while increasing if β is positive.

3 Results and Analysis

3.1 Spatial distribution of annually-averaged PAR

Spatial distribution of perennial average of annually-averaged PAR over China for 1961–2007 is presented in Figure 2. The spatial distribution of PAR is complex and inhomogeneous across China, with lower PAR in the eastern and southern parts of China and higher PAR in the western part. Annually-averaged PAR across China in recent 50 years ranges from 17.7 mol m^{-2} d^{-1} to 39.5 mol m^{-2} d^{-1}, with maximum value of above 35 mol m^{-2} d^{-1} in the southwestern part of Qinghai-Tibet Plateau and minimum value of below 20

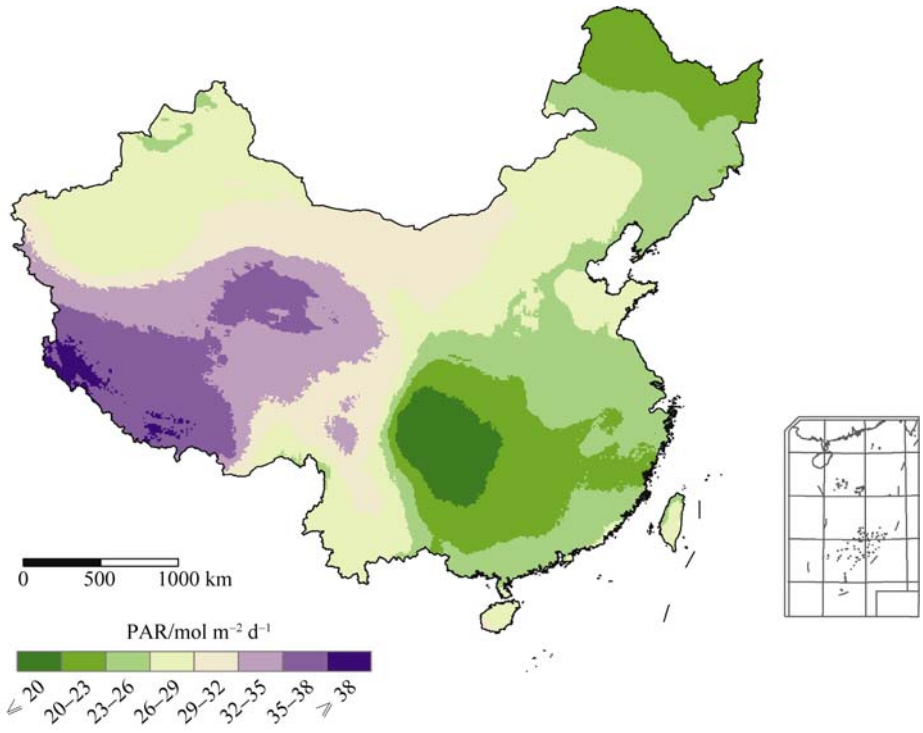

Figure 2 Spatial distribution of annually-averaged PAR over China (averaged for 1961–2007)

mol $m^{-2} d^{-1}$ in Sichuan Basin. In the eastern part of China, low PAR, ranging from 20 mol $m^{-2} d^{-1}$ to 23 mol $m^{-2} d^{-1}$, exists in the south of the Yangtze River Basin and PAR increases southward and northward, with a range of 23–29 mol $m^{-2} d^{-1}$ in North China and 23–26 mol $m^{-2} d^{-1}$ in South China, and then gradually decreases towards Northeast China. In the western part of China, annually-averaged PAR increases from north to south, with low value of below 29 mol $m^{-2} d^{-1}$ in Tarim Basin and Junggar Basin, and with a range of 26–32 mol $m^{-2} d^{-1}$ in Inner Mongolia. PAR in the Qinghai-Tibet Plateau is about 1/3 higher than that in Xinjiang and nearly as higher again as that in Sichuan Basin.

3.2 Interannual variability of annually- and seasonally-averaged PAR

Time series of annual departures of mean PAR for China as a whole (Figure 3) are derived from annually- and seasonally-averaged PAR spatial data for 1961–2007, by means of alge-

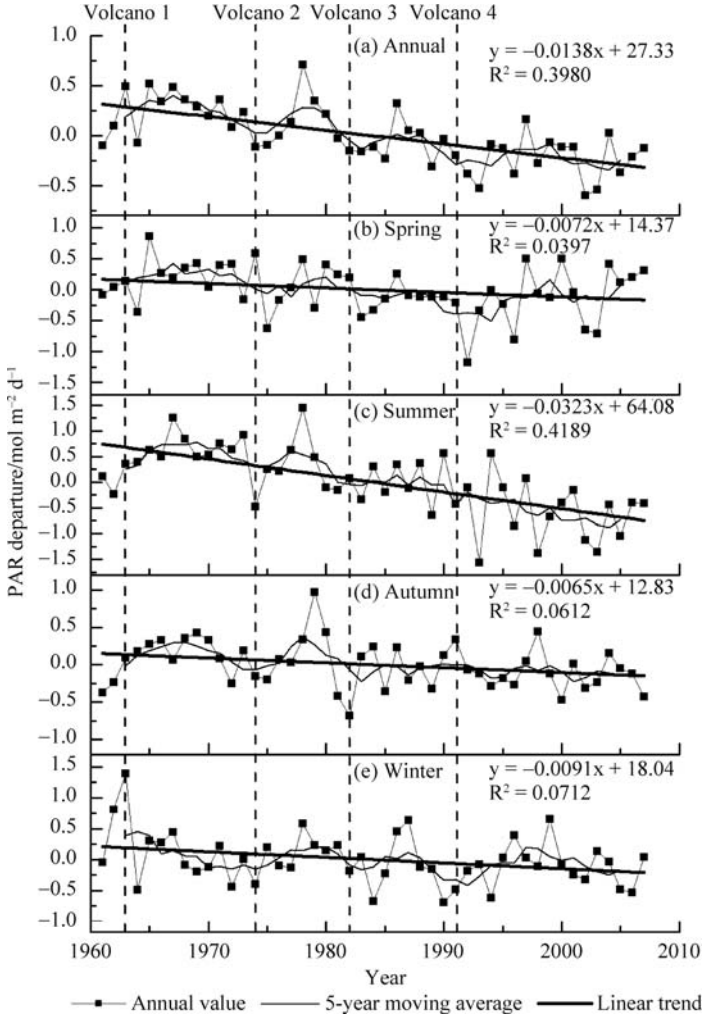

Figure 3 All-China time series of annual departures of annually- (a) and seasonally-averaged (b-e) PAR for 1961–2007. Dashed lines denote time of volcanic eruptions. Volcano 1: Agung (8.3°S, 115.5°E); Volcano 2: Fuego (14.5°N, 125.5°E); Volcano 3: El-Chichon (17.3°N, 93.2°W); Volcano 4: Pinatubo (15.09°N, 120.2°E)

braic operation on GIS platform. Annually-averaged PAR decreases slowly from 1961 to 2007, with a mean decreasing amplitude of 0.138 mol m^{-2} d^{-1}/10a. It decreases obviously before the 1990s with almost above average, while the descending speed slows down after the 1990s. Maximum value of annually-averaged PAR in recent 50 years occurs in 1978, 0.71 mol m^{-2} d^{-1} higher than perennial average, and four low-value troughs occur around 1964, 1975, 1983 and 1993, respectively. The 5-year moving average curves of annual departure of annually-averaged PAR indicate that annually-averaged PAR declines visibly with a fluctuant process in recent 50 years, with an undulation period of quasi-10-year (Figure 3a).

The annual departure curves of seasonally-averaged PAR are presented in Figures 3b-e. The most obvious decline happens in summer with a decreasing amplitude of 0.323 mol m^{-2} d^{-1}/10a; while the declining trends in other seasons are not significant, with decreasing amplitudes of 0.072 mol m^{-2} d^{-1}/10a, 0.065 mol m^{-2} d^{-1}/10a, and 0.091 mol m^{-2} d^{-1}/10a, respectively. Comparing to other seasons, the annual departure curve of summer-averaged PAR is most similar to that of annually-averaged PAR, and also declines visibly with a fluctuant process with maximum value in 1978, 1.45 mol m^{-2} d^{-1} higher than perennial average (Figure 3c). Therefore, PAR undulation in summer plays the most important role in the interannual variability of PAR. Furthermore, it can be seen from the annual departure curves of four seasons that the decreasing speed slows down after the 1990s, most obvious in spring and autumn, even having a upward trend in spring (Figure 3b).

On the whole, annually- and seasonally-averaged PAR decline visibly in recent 50 years, with a faster descending speed before the 1990s than after that; and the changing amplitudes among four seasons are different, with maximum dropping in summer; and PAR undulation in summer plays the most important role in the interannual variability of PAR.

3.3 Spatial distribution of interannual variability of annually- and seasonally-averaged PAR

Annually- and seasonally-averaged PAR spatial data for 1961–2007 are analyzed by each pixel using Mann-Kendall trend analysis method, and the results show that obvious differences in different regions and seasons exist in the interannual variability of PAR across China in recent 50 years (Figure 4). The analyzed results of temporal variation of annually-averaged PAR indicate that annually-averaged PAR declines significantly (α=0.05) in most parts of China (56.4% of total area) and increases significantly in small parts of China (12.5% of total area) (Figure 4a). In the eastern part of China, annually-averaged PAR declines significantly in most areas and decreasing amplitudes exceed 1.5%/10a in North China, South China and East China. In the western part of China, annually-averaged PAR declines significantly in Xinjiang and the southern part of Qinghai-Tibet Plateau, with relative low decreasing amplitudes of below 1.5%/10a; however, it increases significantly in the northern part of Qinghai-Tibet Plateau, with increasing amplitudes of 0–3%/10a.

The analysis results of temporal variation of seasonally-averaged PAR (Figures 4b-e) indicate that temporal variation of PAR differs among four seasons, except for in different regions. The patterns of spatial distribution of annually- and seasonally-averaged PAR are nearly the same, but in changing amplitudes and regional extents. Changing amplitudes and

regional extents vary with season, greater in summer and winter than spring and autumn, with the most in summer. It can be seen from Figure 4c that spatial distribution of interannual changing rates of summer-averaged PAR differs most obviously among four seasons. In the eastern part of China, except Northeast China, we found a remarkable decrease in PAR, with the highest decreasing amplitude of 4.5%–6%/10a in Yangtze River Basin and decreasing amplitudes diminishing southward and northward. Decreasing amplitudes range from 1.5%/10a to 4.5%/10a in North China, and from 1.5%/10a to 3%/10a in South China. In the western part of China, variation characteristics of seasonally-averaged PAR are the same as those of annually-averaged PAR, except that regional extents where PAR increases significantly diminish. Spatial distribution of interannual changing rates of winter-averaged PAR indicates (Figure 4e) that areas of high decreasing amplitudes are the same as those for summer, situated in Yangtze Rive Basin, but with smaller decreasing amplitudes of 3%–4.5%/10a. South China turns from significantly decreasing areas in summer into no trend areas in winter, and decreasing amplitudes in Xinjiang increase to 1.5%–4.5%/10a. Comparing to summer and wither, changing amplitudes and regional extents of interannual variability of PAR in spring and autumn turn down (Figures 4b and 4d).

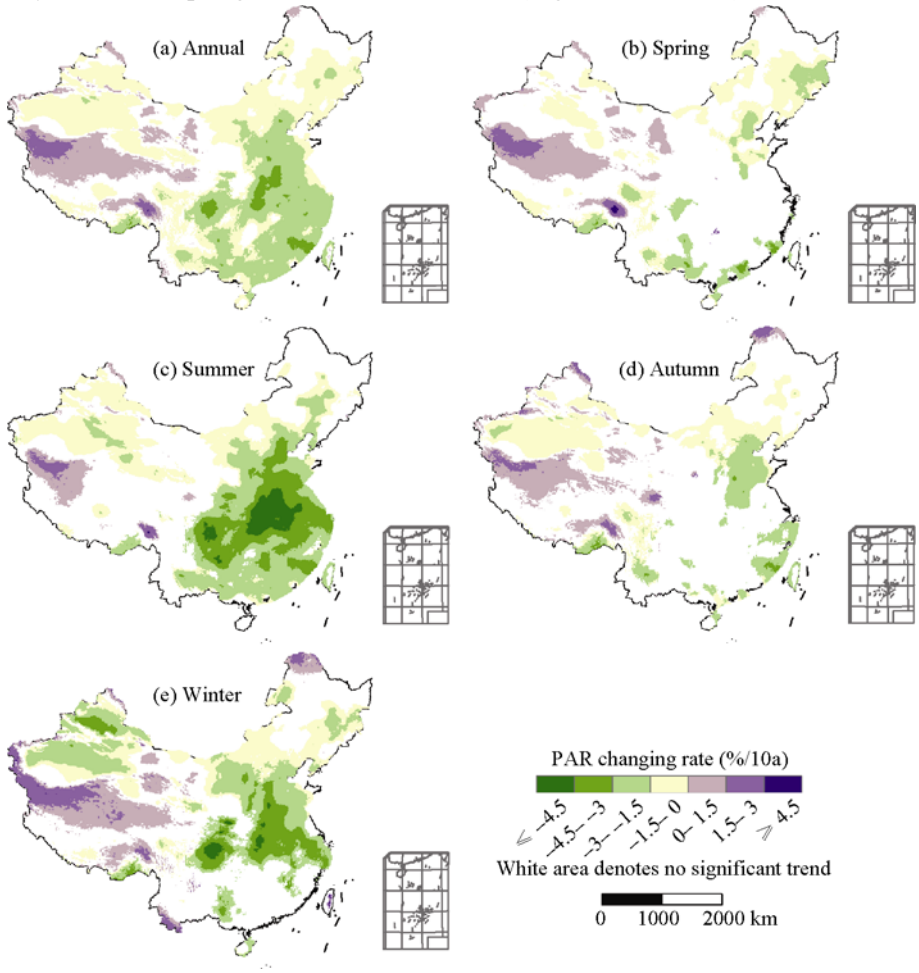

Figure 4 Spatial distribution of changing rates of annually- (a) and seasonally-averaged (b-e) PAR over China for 1961–2007 (%/10a, α=0.05).

In view of differences of interannual variability of PAR among different periods in recent 50 years (Figure 3), PAR spatial data for 1961–2007 are divided into three periods for further analysis (period 1: 1961–1975, period 2: 1976–1990, period 3: 1991–2007). Annually-averaged and typical summer- and winter-averaged PAR for these three periods are examined to explore spatial distributions of interannual variability of annually- and seasonally-averaged PAR in different periods. (1) Spatial distribution of interannual variability of annually-averaged PAR is presented in Figures 5a-c. In the period 1, most of significantly decreasing areas are located in the Middle-Lower Yangtze River with decreasing amplitudes of 5%–10%/10a, while most of significantly increasing areas are located in the eastern and northwestern parts of Tibet with increasing amplitudes of 5%–10%/10a. In the period 2, significantly decreasing areas disperse, situated in some areas of Loess Plateau, Yunnan, Heilongjiang, Xinjiang, *etc.*; the Middle-Lower Yangtze River has no trend, and significantly increasing areas are intensively located in the northwestern part of Qinghai-Tibet Plateau. In the period 3, significantly decreasing areas diminish, mainly situated in North China and the western part of Tibet, but significantly increasing areas expand obviously, typically situated in the northern part of Heilongjiang with increasing amplitudes of above 10%/10a. (2) Spatial distribution of interannual variability of summer-averaged PAR differs very

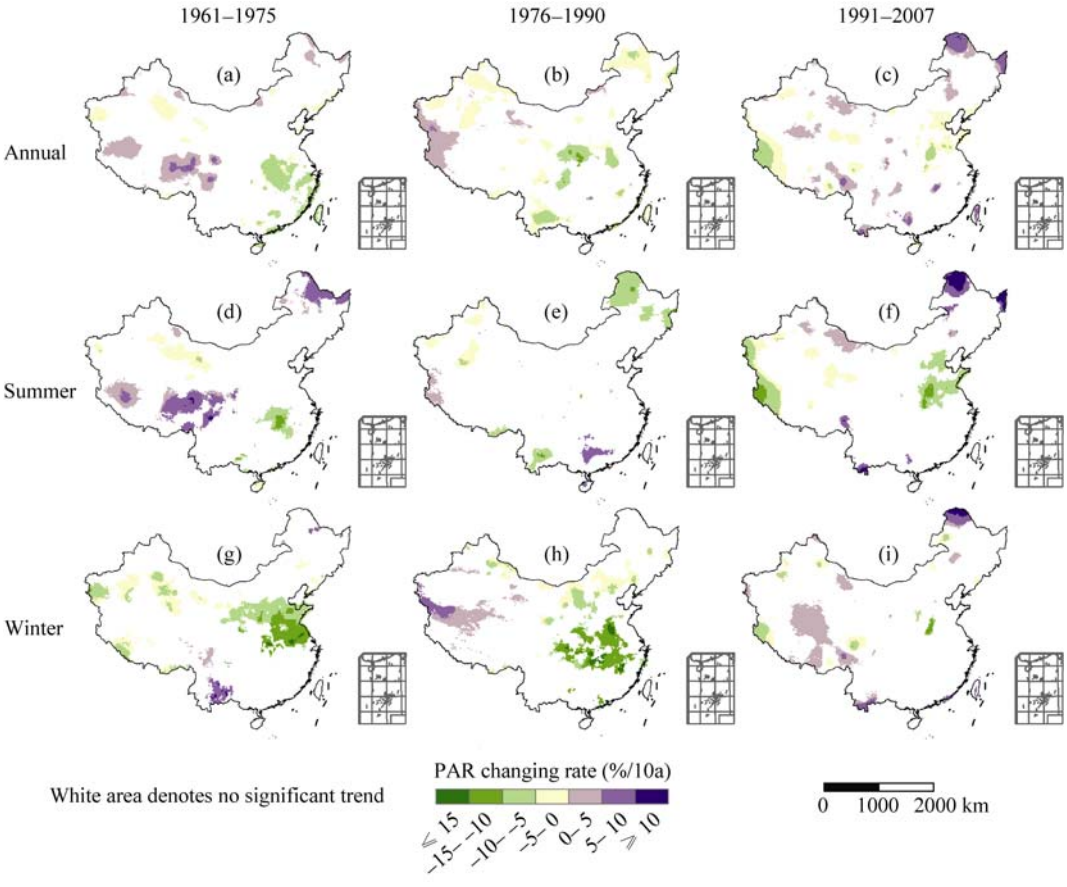

Figure 5 Spatial distribution of changing rates of annually- and seasonally-averaged PAR over China in different periods (%/10a, α=0.05).

obviously (Figures 5d-f). The eastern part of Qinghai-Tibet Plateau is main significantly increasing areas with increasing amplitudes of above 5%/10a in period 1, but it shows no obvious trend in periods 2 and 3. Significantly decreasing areas are located in Jiangxi in period 1, in the northern part of Northeast China in period 2, and in North China and the western part of Tibet in period 3. (3) Spatial distribution of interannual variability of winter-averaged PAR indicates (Figures 5g-i) that significantly decreasing areas are mainly located in North China Plain, while significantly increasing areas are located in the southern part of Yunnan in period 1. In period 2, significantly decreasing areas are located in North China and Yangtze Rive Basin, while significantly increasing areas are located in the northwestern part of Tibet. In period 3, there is almost no significantly decreasing area, and significantly increasing areas are located in the northern part of Heilongjiang and the mid-eastern part of Tibet.

On the whole, there are two evident features of interannual variability of annually- and seasonally-averaged PAR over China: from the aspect of spatial scale, temporal variation characteristics of PAR is distinct in the eastern part of China from that in the western part, with wider regional extents and larger changing amplitudes in the east than in the west; from the aspect of seasonal scale, changing amplitudes and regional extents in summer and winter exceed those in spring and autumn. In addition, the comparative analysis among three periods reveals that PAR shows distinct variation characteristics among different periods, and that the descending speed of PAR is faster before the 1990s, after which the speed slows down, even having a upward trend.

3.4 Cause analysis of variability of PAR

Many factors influence spatio-temporal variation characteristics of PAR, including extraterrestrial radiation, cloud cover, aerosols, etc.

(1) Extraterrestrial radiation is the basis of incident solar radiation that earth surface receives. It is the initial calculation parameter for PAR and directly influences the amount of PAR. However, extraterrestrial radiation is relatively stable in that the change of solar constant is about 1.36 W m^{-2} (changing rate of only 0.1%), which can be revealed by satellite observatory data in recent decades (Lean, 1997).

(2) Cloud is an important obstacle preventing solar radiation from reaching earth surface, and increasing cloud amount would lead to decreasing PAR. It can be known from temporal variation analysis of PAR in this paper that PAR declines significantly in most parts of China in recent 50 years, but cloud amount also declines in most parts of China in recent decades as reported by many research work. That is to say, the change of cloud amount can not account for the significant decline of PAR in recent 50 years (Li *et al.*, 1998; Zeng and Yan, 1993). Therefore, the change of cloud amount is not a key factor influencing the temporal variability of PAR over China in recent 50 years.

(3) The increase of aerosol would lead to a decrease of direct fraction and an increase of diffuse fraction of PAR. However, the total amount of incident PAR reaching earth surface decreases in that the amount of diffuse PAR is generally much smaller than direct PAR. The increase of aerosol comes from two sources: volcanic eruptions and anthropogenic activities. In recent 50 years, PAR declines with a fluctuant process and troughs in the process are closely related to major volcanic eruptions, including Agung volcano in 1963 (8.3°S,

115.5°E), Fuego volcano in 1974 (14.5°N, 125.5°E), El-Chichon volcano in 1982 (17.3°N, 93.2°W) and Pinatubo volcano in 1991 (15.09°N, 120.2°E) (Figure 3). It can be seen from Figure 3a that four troughs in the declining process of PAR occur in 1–2 year after big volcanic eruptions. Pinatubo volcano erupted in 1991, the most violent one in recent 100 years, ejected about 14–20 Tg (1 Tg = 10^{12} g) sulfate aerosol into stratosphere, increasing aerosol to the maximum in low latitude region in three months and in middle latitude region of Northern Hemisphere in May or June, 1992 (Zha, 1996). The ejected aerosol directly resulted in a decrease in the amount of incident solar radiation (Stowe *et al.*, 1992; Minnis *et al.*, 1993), which give the reason why annually-averaged PAR is at relatively low values in three consecutive years after 1991 (Figure 3a). Another important reason for temporal variability of PAR in recent 50 years is that the rapid development of global economy, the population explosion and the large-scale use of fossil fuels lead to a great increase in atmospheric pollutants, which lowers down atmospheric transparency. Accordingly, temporal dynamics of PAR with a fluctuant declining process in recent 50 years attribute to the increase of aerosol from volcano eruptions and anthropogenic activities. The latter is the key factor that contributes to the steadily declining process of PAR, while the former accounts for the fluctuant process of PAR. The combination of these two influencing factors leads to decreasing PAR with a fluctuant process in recent 50 years. Furthermore, it can be seen from Figure 3 that there is a quasi-10-year period in the fluctuation of PAR, which is similar to 11-year solar cycle, that is, the fluctuation of PAR is likely associated with solar cycle.

Not only does perennial average of PAR has an uneven spatial distribution in recent 50 years (Figure 2), but also interannual changing rates of PAR differ obviously between the eastern and western parts of China (Figure 4). The uneven spatial distribution of perennial average of PAR attributes to many influencing factors, such as geographic location, topography and atmospheric circulation. PAR in Qinghai-Tibet Plateau is higher than that in low elevation areas of the same latitudes, with two reasons accounting for this phenomenon. On the one hand, a higher elevation of Qinghai-Tibet Plateau accompanies with a shorter distance from the top of atmosphere to earth surface, that is, PAR is less weakened in the process of radiation transfer. One the other hand, a higher elevation leads to thinner air, thus PAR is less influenced by atmosphere. Sichuan Basin and Middle-Lower Yangtze River are influenced by monsoon climate, which leads to more amount of cloud and shorter actual sunshine duration, and therefore PAR in these areas is lower than other areas in China. Additionally, lower PAR in these areas is also caused by increasingly serious air pollution that is not easy to disperse under the control of subtropical high in summer. The differences in spatial distribution of interannual changing rates of PAR between the eastern and western parts of China are mainly associated with the differences in economy and population. In recent 50 years, with the development of economy and the explosion of population in the eastern part of China, air pollution is more serious and the increasing rate of aerosol is greater, compared to those in the western part of China. Therefore, interannual changing rates of PAR in the eastern part of China are greater than those in the western part.

4 Conclusions

Based on long-term measurement data of weather/ecological stations over China, we calcu-

lated and produced annually- and seasonally-averaged PAR spatial data from 1961 to 2007, using climatological calculations and spatialization techniques. Moreover, the spatio-temporal variation characteristics of annually- and seasonally-averaged PAR spatial data in China in recent 50 years were analyzed with Mann-Kendall trend analysis method and GIS spatial analysis technique at temporal and spatial scale. Several conclusions are derived as below:

(1) The spatial distribution of PAR is complex and inhomogeneous across China, with maximum value in the southwestern part of Qinghai-Tibet Plateau and minimum value in Sichuan Basin. Annually-averaged PAR over China in recent 50 years ranges from 17.7 mol m^{-2} d^{-1} to 39.5 mol m^{-2} d^{-1}. In the western part of China, annually-averaged PAR increases from north to south. In the eastern part of China, low PAR exists in the south of the Yangtze River Basin and PAR increases southward and northward, and then gradually decreases towards Northeast China.

(2) PAR is averaged over China as a whole and both annually- and seasonally-averaged PAR decline obviously with fluctuant processes in recent 50 years, with a mean decreasing amplitude of 0.138 mol m^{-2} d^{-1}/10a and a faster decreasing speed before the 1990s than after that. The changing amplitudes among four seasons are different, with maximum dropping in summer.

(3) The analysis by each pixel shows that PAR declines significantly in most parts of China. The changing trend in the eastern part of China is more obvious than that in the western part, and summer and winter play more important roles in the interannual variability of PAR. The interannual changing rates of PAR in a certain region are different among four seasons, and spatial distributions vary with season as well. North China is always a decreasing zone among four seasons, while the northwest of Qinghai-Tibet Plateau turns to be an increasing zone among four seasons.

(4) The spatial distributions of the interannual variability of PAR among different periods are not the same in recent 50 years. The interannual variability of PAR in a certain region is different not only among four seasons, but also among different periods. As a whole, the descending speed of PAR is faster and decreasing/increasing areas are more concentrated before the 1990s, after which the speed slows down and decreasing/increasing areas disperse.

This paper aims to explore spatio-temporal dynamic characteristics of long-term PAR spatial data using GIS spatial analysis techniques and time-varying analyzing method. By means of visualization, quantifying, and truly reflecting local features provided by GIS spatial analysis techniques, spatial pattern and temporal dynamics of PAR over China are examined deeply in pixel and regional scales, realizing a comprehensive study of spatio-temporal variation characteristics of PAR in complex geographic environments of China. The deficiencies of GIS spatial analysis techniques, including authenticity of original data and veracity of spatial interpolation method, may bring about a certain uncertainties in eventual results (Gong and Wang, 2002). However, this paper focuses on spatio-temporal variation analysis of PAR at regional scale, so the derived results are able to represent general variation characteristics of PAR, which will greatly promote the study of ecosystem processes at regional scale, including spatio-temporal variability and pattern of ecosystem production and underlying driving mechanisms.

References

Almorox J, Hontoria C, 2004. Global solar radiation estimation using sunshine duration in Spain. *Energy Conversion and Management*, 45(9/10): 1529–1535.

Ångstrøm A, 1924. Solar and terrestrial radiation. *Quarterly Journal of the Royal Meteorological Society*, 50: 121–125.

Bai Jianhui, Wang Gengchen, 2004. The calculating method of photosynthetically active radiation in the Inner Mongolia grassland. *Research of Environmental Sciences*, 17(6): 15–18. (in Chinese)

Cao M K, Prince S D, Tao B *et al*., 2005. Regional pattern and interannual variations in global terrestrial carbon uptake in response to changes in climate and atmospheric CO_2. *Tellus Series B-Chemical and Physical Meteorology*, 57(3): 210–217.

Dye D G, 2004. Spectral composition and quanta-to-energy ratio of diffuse photosynthetically active radiation under diverse cloud conditions. *Journal of Geophysical Research-Atmospheres*, 109(D10).

Gong Daoyi, Wang Shaowu, 2002. Uncertainties in the global warming studies. *Earth Science Frontiers*, 57(6): 631–638. (in Chinese)

Graham E A, Mulkey S S, Kitajima K *et al*., 2003. Cloud cover limits net CO_2 uptake and growth of a rainforest tree during tropical rainy seasons. *Proceedings of the National Academy of Sciences of the United States of America*, 100(2): 572–576.

He Honglin, Liu Jiyuan, Yu Guirui, 2004a. Study on spatialization of solar radiation in China [D]. Beijing: Institute of Geographic Sciences and Natural Resources Research, Chinese Academy of Sciences. (in Chinese)

He Honglin, Yu Guirui, Liu Xinan *et al*., 2004b. Study on spatialization technology of terrestrial eco-information in China (II). *Solar radiation. Journal of Natural Resources*, 19(5): 679–687. (in Chinese)

He Honglin, Yu Guirui, Niu Dong, 2003. Method of global solar radiation calculation on complex territories. *Resources Science*, 25(1): 78–85. (in Chinese)

Herber A, Thomason L W, Dethloff K *et al*., 1996. Volcanic perturbation of the atmosphere in both polar regions: 1991–1994. *Journal of Geophysical Research-Atmospheres*, 101(D2): 3921–3928.

Hijmans R J, Cameron S E, Parra J L *et al*., 2005. Very high resolution interpolated climate surfaces for global land arras. *International Journal of Climatology*, 25: 1965–1978.

Hu B, Wang Y, Liu G, 2007. Spatiotemporal characteristics of photosynthetically active radiation in China. *Journal of Geophysical Research*, 112(D14106).

Hutchinson M F, 1991. The application of thin plate smoothing splines to continent-wide data assimilation. In: Jasper J D ed. Data Assimilation Systems. BMRC Research Report Number 27, Bureau of Meteorology, Melbourne, Australia.

Hutchinson M F, 1995. Interpolating mean rainfall using thin plate smoothing splines. *International Journal of Geographical Information Science*, 9: 385–403.

Hutchinson M F, 2002. ANUSPLIN Version 4.2 User Guide. Centre for Resource and Environment Studies. Canberra: Australian National University.

Jacovides C P, Timvios F S, Papaioannou G *et al*., 2004. Ratio of PAR to broadband solar radiation measured in Cyprus. *Agricultural and Forest Meteorology*, 121(3/4): 135–140.

Lean J, 1997. The sun's variable radiation and its relevance for earth. *Annual Review of Astronomy and Astrophysics*, 35: 33–67.

Li Xiaowen, Li Weiliang, Zhou Xiuji, 1998. Analysis of the solar radiation variation of China in recent 30 years. *Quarterly Journal of Applied Meteorology*, 9(1): 24–31. (in Chinese)

Lin Zhonghui, Mo Xingguo, Li Hongxuan, 2002. Comparison of three spatial interpolation methods for climate variables in China. *Acta Geographica Sinica*, 57(1): 47–56. (in Chinese)

Liu Xinan, Fan Liaosheng, Wang Yanhua *et al.*, 2002. The calculation methods and distributive character of solar radiation in Liaoning province. *Resources Science*, 24(1): 82–87. (in Chinese)

Louche A, Notton G, Poggi P *et al.*, 1991. Correlations for direct normal and global horizontal irradiation on a French Mediterranean site. *Solar Energy*, 46(4): 261–266.

Minnis P, Harrison E F, Stowe L L *et al.*, 1993. Radiative climate forcing by the Mount Pinatubo eruption. *Science*, 259(5100): 1411–1415.

Monteith J L, 1972. Solar-radiation and productivity in tropical ecosystems. *Journal of Applied Ecology*, 9(3): 747–766.

Monteith J L, 1977. Climate and efficiency of crop production in Britain. *Philosophical Transactions of the Royal Society of London Series B-Biological Sciences*, 281(980): 277–294.

Robock A, 2000. Volcanic eruptions and climate. *Reviews of Geophysics*, 38(2): 191–219.

Ross J, Sulev M, 2000. Sources of errors in measurements of PAR. *Agricultural and Forest Meteorology*, 100(2/3): 103–125.

Stowe L L, Carey R M, Pellegrino P P, 1992. Monitoring the Mt. Pinatubo aerosol layer with NOAA/11 AVHRR data. *Geophysical Research Letter*, 19(2): 159–162.

Sun Zhi'an, Shi Junrong, Weng Duming, 1992. A further research on the climatological calculation method of the global solar radiation over China. *Journal of Nanjing Institute of Meteorology*, 15(2): 21–29. (in Chinese)

Tong Chengli, Zhang Wenju, Tang Yang *et al*., 2005. Estimation of daily solar radiation in China. *Chinese Journal of Agrometeorology*, 26(3): 165–169. (in Chinese)

Udo S O, Aro T O, 1999. Global PAR related to global solar radiation for central Nigeria. *Agricultural and Forest Meteorology*, 97(1): 21–31.

Van P, Sanchez-Azofeifa G, 2005. Mapping PAR using MODIS atmosphere products. *Remote Sensing of Environment*, 94(4): 554–563.

Wei Fengying, 2007. Modern Statistical Diagnosis and Forecasting Techniques for Climate. 2nd ed. Beijing: China Meteorological Press, 63–66. (in Chinese)

Yu Guirui, He Honglin, Liu Xinan *et al*., 2004. Atlas for Spatialized Information of Terrestrial Ecosystem in China: Volume of Climatological Elements. Beijing: China Meteorological Press. (in Chinese)

Yu P S, Yang T C, Wu C K, 2002. Impact of climate change on water resources in southern Taiwan. *Journal of Hydrology*, 260(1–4): 161–175.

Zeng Zhaomei, Yan Zhongwei, 1993. An analysis of cloudiness in China during 1950–1988. *Scientia Atmospherica Sinica*, 17(6): 688–696. (in Chinese)

Zha Liangsong, 1996. A study on spatial and temporal variation of solar radiation in China. *Scientia Geographica Sinica*, 16(3): 232–237. (in Chinese)

Zhang X, Zhang Y, Zhou Y, 2000. Measuring and modelling photosynthetically active radiation in Tibet Plateau during April–October. *Agricultural and Forest Meteorology*, 102(2/3): 207–212.

Zhang Xiangzhou, Zhang Yiguang, Zhou Yunhua, 1997. Climatological estimation of photosynthetically active quantum value on Qinghai-Xizang Plateau from April to October. *Acta Geographica Sinica*, 52(4): 361–365. (in Chinese)

Zhang Yunlin, Qin Boqiang, 2002. The basic characteristic and climatological calculation of the photosynthetically available radiation in Taihu region. *Acta Energiae Solaris Sinica*, 23(1): 118–123. (in Chinese)

Zhao Ji, Chen Chuankang, 1999. China Geography. Beijing: Higher Education Press, 361–363. (in Chinese)

Zhou Yunhua, Xiang Yueqin, Luan Lukai, 1996. Climatological estimation of quantum flux densities. *Acta Meteorologica Sinica*, 54(4): 447–455. (in Chinese)